Nanoscale

PAPER

Cite this: *Nanoscale*, 2016, **8**, 5537

Fatty acids and small organic compounds bind to mineralo-organic nanoparticles derived from human body fluids as revealed by metabolomic analysis†

Jan Martel,‡[a,b] Cheng-Yeu Wu,‡[a,b,c] Cheng-Yu Hung,‡[d,e,f] Tsui-Yin Wong,[a,b,g] Ann-Joy Cheng,[h] Mei-Ling Cheng,[d,e,f] Ming-Shi Shiao[d,e,f] and John D. Young[a,b,i,j]

Received 17th November 2015,
Accepted 7th January 2016

DOI: 10.1039/c5nr08116e

www.rsc.org/nanoscale

Nanoparticles entering the human body instantly become coated with a "protein corona" that influences the effects and distribution of the particles *in vivo*. Yet, whether nanoparticles may bind to other organic compounds remains unclear. Here we use an untargeted metabolomic approach based on ultra-performance liquid chromatography and quadruple time-of-flight mass spectrometry to identify the organic compounds that bind to mineral nanoparticles formed in human body fluids (serum, plasma, saliva, and urine). A wide range of organic compounds is identified, including fatty acids, glycerophospholipids, amino acids, sugars, and amides. Our results reveal that, in addition to the proteins identified previously, nanoparticles harbor an "organic corona" containing several fatty acids which may affect particle-cell interactions *in vivo*. This study provides a platform to study the organic corona of biological and synthetic nanoparticles found in the human body.

Introduction

Our earlier studies have shown that mineral nanoparticles (NPs) form spontaneously in human body fluids when the concentrations of calcium, carbonate and phosphate ions exceed saturation.[1–16] These mineral NPs have helped us to solve a major scientific controversy surrounding the existence of the so-called nanobacteria—small mineralized entities described earlier as the smallest microorganisms on earth and the possible cause of several human diseases.[17–19] In contrast to earlier claims, our results have shown that nanobacteria are actually non-living mineralo-protein NPs that possess biomimetic properties.[1–16] Surprisingly, these mineralo-protein NPs have been shown to form in the bones and teeth of vertebrates as well as in ectopic calcifications, suggesting that these particles may represent mineral precursors associated with both physiological and pathological mineralization processes (recently reviewed[13]).

Chemically synthesized and naturally formed NPs entering the human body are instantly coated with proteins present in biological fluids. These proteins, which form the "protein corona", have been shown to affect the distribution and effects of NPs in the body.[20–26] A recent study by Tenzer *et al.* reported that the protein corona of silica and polystyrene NPs modulates the level of particle-induced hemolysis, thrombocyte activation, and endothelial cell death.[27] Similarly, the protein corona of synthetic polymer particles affects particle uptake by human macrophages,[27–29] a process which may influence particle clearance *in vivo*. Another study showed that removal of glycan moieties on corona proteins increases particle-cell adhesion and particle uptake by macrophages.[30] Deciphering the molecules that bind to NPs and the factors influencing the interactions may provide critical information about the effects of nanomaterials in the human body.

We developed earlier a comprehensive approach to study the protein corona of mineralo-protein NPs formed in human body fluids[7] and found that a wide range of proteins interact

[a]*Laboratory of Nanomaterials, Chang Gung University, Taoyuan 33302, Taiwan. E-mail: dingeyoung@hotmail.com*
[b]*Center for Molecular and Clinical Immunology, Chang Gung University, Taoyuan 33302, Taiwan*
[c]*Research Center of Bacterial Pathogenesis, Chang Gung University, Taoyuan 33302, Taiwan*
[d]*Healthy Aging Research Center, Chang Gung University, Taoyuan 33302, Taiwan*
[e]*Department of Biomedical Sciences, College of Medicine, Chang Gung University, Taoyuan 33302, Taiwan*
[f]*Metabolomics Core Laboratory, Chang Gung University, Taoyuan 33302, Taiwan*
[g]*Center for General Education, Chang Gung University of Science and Technology, Chiayi 61363, Taiwan*
[h]*Graduate Institute of Medical Biotechnology, Department of Medical Biotechnology and Laboratory Science, Chang Gung University, Taoyuan 33302, Taiwan*
[i]*Biochemical Engineering Research Center, Ming Chi University of Technology, New Taipei City 24301, Taiwan*
[j]*Laboratory of Cellular Physiology and Immunology, Rockefeller University, New York, NY 10021, USA*

†Electronic supplementary information (ESI) available. See DOI: 10.1039/c5nr08116e

‡These authors contributed equally to this work.

with these particles, including calcification inhibitors, coagulation factors, complement proteins, immune regulators, and protease inhibitors. While research suggests that synthetic NPs exposed to human plasma may bind to compounds such as cholesterol, triglycerides and phospholipids,[31] it remains unclear whether biological NPs that form in body fluids generally bind to organic compounds. It is also unknown whether such non-protein compounds may influence physiological processes, including the conversion of mineralo-organic NPs to crystalline biofilms,[16] the interactions between these particles and immune cells,[10] or the formation of mineralo-organic NPs in human tissues.[15] Here, we present a liquid chromatography-mass spectrometry (LC-MS)-based, untargeted metabolomic approach to analyze the low-molecular-weight (LMW) metabolites associated with mineral NPs derived from human and bovine body fluids.

Experimental procedure

Preparation of particles

The use of human body fluids was approved by the Institutional Review Board of Chang Gung Memorial Hospital (Taoyuan, Taiwan). Written informed consent was obtained from the volunteers. Human blood was withdrawn from healthy individuals and serum was prepared as before.[2] Saliva and urine samples were obtained from healthy human volunteers. Human plasma was collected into tubes containing sodium heparin (Becton & Dickinson). Human serum (HS), plasma, saliva, urine, and commercial fetal bovine serum (FBS; Biological Industries) were sterilized by successive filtration through 0.2 μm and 0.1 μm-pore membranes (Pall Corporation).

Carbonate apatite NPs were prepared by adding both $CaCl_2$ and NaH_2PO_4 at a final concentration of 3 mM each to Dulbecco's modified Eagle's medium (DMEM; Gibco) containing a body fluid (*i.e.*, HS, plasma, saliva, urine, or FBS) at a concentration of 10% (v/v) in a final volume of 1 mL. The samples were incubated in cell culture conditions with gentle end-to-end agitation overnight, followed by centrifugation at 16 000*g*, washing twice with DMEM, and resuspension in 50 μL of a 1 : 3 mixture of 200 mM EDTA and 100% methanol. Three volumes of a 1 : 3 mixture of 0.4 M HCl and 100% methanol were added to further dissolve the particles by acidification. The solution was sonicated for 30 min at 37 °C. Metabolites were pelleted and dried in a vacuum centrifuge and resuspended in 100 μL of 80% methanol. The samples were centrifuged at 16 000*g* for 5 min to remove insoluble material and the clear supernatant was collected for LC-MS analysis. In some experiments, serum that was first treated with 0.5% porcine trypsin (Sigma) at 37 °C overnight was used to prepare mineralo-organic NPs as above.

Serum granules were obtained as before[3] by incubating filtered HS or FBS (38 mL) with agitation overnight at room temperature, followed by ultra-centrifugation at 140 000*g* at 4 °C for 2 h and washing twice using the same centrifugation step. The particles were treated with EDTA and HCl, prior to preparation for LC-MS analysis as described above.

Polystyrene NPs (mean particle size of 50 and 100 nm; Uni-Onward) were incubated into 10% HS for 1 day with end-to-end agitation at room temperature, prior to centrifugation at 16 000*g* for 30 min at 4 °C. The particles were washed in phosphate buffered saline (PBS) and resuspended in 200 μL of 80% methanol to release organic molecules. The solution was sonicated for 30 min on ice. The particles were pelleted by centrifugation and the supernatant was collected. The supernatant (150 μl) containing the organic compounds was evaporated in a vacuum centrifuge and the organic compounds found in the resulting pellet were redissolved in 200 μl of 5% acetonitrile (ACN; HPLC grade).

Scanning electron microscopy

For scanning electron microscopy (SEM), washed particles were resuspended in double distilled water and deposited on formvar carbon-coated grids (Electron Microscopy Sciences). After drying, the specimens were coated with gold for 90 s and observed using a SEM S-5000 field-emission scanning electron microscope (Hitachi Science Systems).

LC-MS analysis

Deionized water prepared with the Milli-Q water purification system (Millipore) was used to prepare all solutions. Chromasolv grade ACN, methanol, and water solvents were obtained from Fluka. Metabolite standards and ammonium formate (98–100%) were purchased from Sigma. Mass spectrometry analysis was carried out using ultra-performance liquid-chromatography (UPLC) system coupled with time-of-flight mass spectrometry (TOF-MS) (Waters). Chromatographic separation was performed on an Acquity BEH C18 column (Waters; 1.7 μm, 2.1 mm × 100 mm). Column temperature was maintained at 45 °C. For metabolite profiling, solvent A consisted of water and solvent B of ACN, with both solvents containing 0.1% formic acid. Solvent gradient was as follows: 0–1.5 min, 1–98% solvent B; 1.5–5.7 min, 98% solvent B; 5.7–5.8 min, 98–1% solvent B; 5.8–7.5 min, 1% solvent B. A flow rate of 0.5 mL min^{-1} and a volume of 3 μL of sample was used.

Mass spectrometric analysis was performed with the Waters Synapt HDMS system operating in positive and negative-ion ESI mode. The capillary and cone voltage were set at 3000 V (2000 V in ESI^- mode) and 35 V, respectively. Desolvation gas flow rate was set at 700 L h^{-1}, and gas flow was maintained at 25 L h^{-1}. The desolvation and source temperatures were set at 300 °C and 80 °C, respectively. MS data was acquired over a range of m/z of 20 to 990 at a rate of 0.1 scan per s. Data were collected in centroid mode. Sulfadimethoxine was used as a reference compound (m/z of 311.081 in ESI^+ mode and 309.0658 in ESI^- mode). LockSpray frequency was set at 0.5 s and was averaged over 10 scans for correction.

Data analysis

Time-aligned ion features, mono-isotopic neutral mass, retention time, and ion signal intensity were extracted from the raw data using the molecular feature extraction algorithm. Data matrices were determined using the MassLynx software

(Waters). Heat map and PCA diagrams were prepared using MetaboAnalyst.[32]

Metabolite identification

Information on candidate metabolites was obtained from the Human Metabolome Database (http://www.hmdb.ca) and a database maintained in our laboratory based on chemical element composition and mass accuracy. Candidates for MS/MS analysis were selected from the metabolites with high intensity signals in UPLC-MS chromatograms. For further identification, pure metabolite standards were processed through LC-MS using the same conditions as above. MS/MS spectra were collected and confirmed by chemical standards or database from METLIN (http://metlin.scripps.edu/index.php) and LIPID MAPS.

Results

Mineralo-organic NPs were prepared by adding calcium into a cell culture medium (*i.e.*, Dulbecco's modified Eagle's medium, or DMEM) containing a body fluid (serum, saliva, or urine), followed by addition of phosphate ions to induce precipitation of calcium phosphate (see Fig. S1 in the ESI†). We found earlier that the mineralo-organic NPs obtained this way are similar to the mineral particles found in the human body.[4,10,15] Given the physiological relevance of these particles, we decided to use these to study the organic compounds that interact with biological particles. The particles showed round or bacillus-like morphologies, with a size distribution of 20 to 400 nm and partial aggregation (Fig. S2;† see also our previous studies[2–4] for more detailed information on the particles' characteristics). Following incubation and washing steps, the particles were treated with the calcium chelator EDTA and with 0.1 M HCl to favor particle dissolution and the release of bound metabolites. Organic compounds were resuspended in methanol and analyzed using reversed-phase ultra-performance liquid chromatography (UPLC) and quadruple time-of-flight mass spectrometry (QTOF-MS) analysis (Fig. S1†).

LC-MS chromatograms of mineralo-organic NPs prepared in human serum (HS), saliva or urine, and analyzed under the positive mode of electrospray ionization (ESI) showed similar peak profiles, with noticeable variation in peak intensity (Fig. 1A, ESI^+). Mineralo-organic NPs derived from fetal bovine serum (FBS) produced peaks similar to those obtained from human body fluids (Fig. 1A), suggesting that a conserved set of organic compounds may interact with NPs exposed to animal body fluids. We also analyzed mineralo-organic NPs obtained directly from serum, without addition of calcium or phosphate (see Experimental procedure). We observed in a previous study[3] that these mineral particles, which we termed "serum granules", also resemble the mineralo-organic NPs that form in the human body. When analyzed by LC-MS analysis, serum granules showed chromatogram profiles similar to that of mineralo-organic NPs derived following addition of ions into body fluids (described above), an observation which further supports the physiological relevance of our approach. In the ESI negative mode (ESI^-), the mineral particles and serum granules prepared in human or bovine body fluids showed a lower number of peaks compared to the particles analyzed in ESI^+ mode (compare Fig. 1B *vs.* 1A). In addition, a higher degree of similarity was noted for the samples analyzed under ESI^- mode compared to those analyzed with ESI^+ mode (Fig. 1B *vs.* 1A).

A total of 670 metabolite candidates were derived from the ion molecular masses obtained for the various mineralo-organic NP samples analyzed in the present study (Table S1 in the ESI;† this number represents the sum of all candidate compounds identified in ESI^+ and ESI^- modes). A total of 377 candidate metabolites matched to a specific compound name following comparison of ion molecular masses against the Human Metabolome Database (ESI Table S1,† named compounds). On the other hand, several ion molecular masses did not match to any known compounds based on the molecular weight search performed (ESI Table S1,† non-available compound, or "N/A"). The metabolite candidates identified belonged to a wide range of chemical classes, including acylcarnitines, amino acids, aromatic compounds, bile acids, sugars, ecosanoids, glycerolipids, glycerophospholipids (GPLs), mono-glycerophosphocholines (MGCs), peptides, pyridines, saturated and unsaturated fatty acids, sphingolipids, sterols, and vitamins, among others (ESI Table S1,† "Chemical Class" column).

Two strategies were used to validate the metabolites bound to mineralo-organic NPs. The first strategy consisted of comparing the MS spectrum of candidate metabolites with the spectrum of the corresponding pure standard, while the second strategy was based on the selection of ions for further ionization by MS/MS analysis and comparison with the metabolite database. Using these two methods, we confirmed the identification of several metabolites found in association with mineralo-organic NPs (Tables 1 and 2; peak numbers in Fig. 1A and B correspond to the metabolites listed in Tables 1 and 2). Following ranking based on UPLC ion intensity, the main metabolites consisted of the saturated free fatty acids stearic acid (C18:0), palmitic acid (C16:0), myristic acid (C14:0), margaric acid (C17:0), and pentadecanoic acid (C15:0), as well as monoacylglycerols (MGs) and the unsaturated fatty acids oleic acid (C18:1), palmitoleic acid (C16:1), and linolenic acids (C18:3) (Tables 1 and 2). In addition, LMW metabolites such as amino acids (L-phenylalanine and L-leucine), sugars (D-glucose), and lyso-phosphatidylcholines (lyso-PCs) were identified (Tables 1 and 2).

Using the LC-MS/MS methodology described here, we identified several metabolites in serum granules derived from either HS or FBS (ESI Table S1†). The metabolites associated with serum granules were comparable to those found in the mineralo-organic NPs described above (ESI Table S1†), further supporting the biological relevance of the approach used here to study the interaction between organic molecules and biological particles. We also used trypsin-treated serum in order to digest and remove the bulk of proteins of NPs prepared in

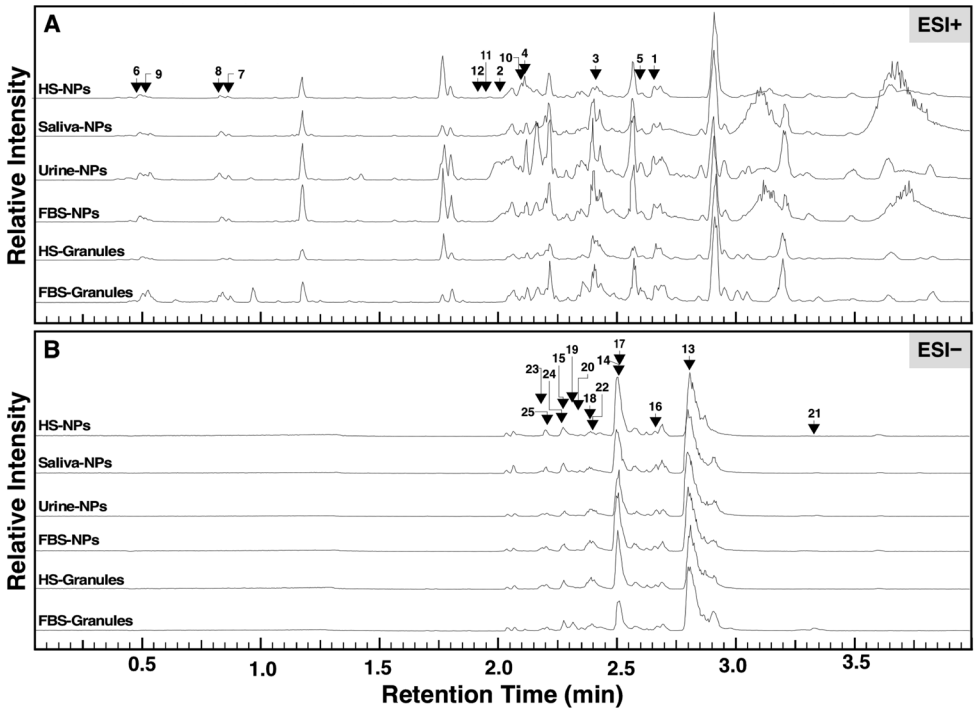

Fig. 1 LC/MS chromatograms of mineralo-organic NPs and serum granules derived from body fluids. Mineralo-organic NPs were prepared by adding $CaCl_2$ and NaH_2PO_4 at 3 mM each in DMEM containing HS, FBS, saliva, or urine, prior to incubation overnight and preparation for LC/MS analysis. Mineral granules derived from HS or FBS were obtained following ultra-centrifugation of serum as described in Experimental procedure. The chromatograms show peaks detected in (A) ESI^+ and (B) ESI^- modes, with peak numbers corresponding to the compounds listed in Tables 1 and 2.

Table 1 List of validated organic compounds identified in mineralo-organic NPs and serum granules in the ESI^+ mode

#	Compound	ID number	Formula	RT	*m/z*	HS-NPs	Saliva-NPs	Urine-NPs	FBS-NPs	HS-Gr.	FBS-Gr.
1	MG (C18:0)	HMDB11535	$C_{21}H_{42}O_4$	2.64	359.3134	939.2	1660.7	1512.5	1374.5	1782.0	1226.9
2	MG (C18:2)	HMDB11538	$C_{21}H_{38}O_4$	2.08	355.2828	813.2	1329.1	1583.6	1037.8	1016.4	934.4
3	MG (C16:0)	HMDB11564	$C_{19}H_{38}O_4$	2.41	331.2822	905.9	1133.9	1169.1	1052.9	1114.7	893.2
4	Lyso-PC (C16:0)	HMDB10382	$C_{24}H_{50}NO_7P$	2.10	496.3406	1884.1	9.3	7.8	695.9	371.3	169.9
5	Stearamide	HMDB34146	$C_{18}H_{37}NO$	2.59	284.2947	334.3	624.4	584.3	505.7	570.4	1036.8
6	D-Glucose	HMDB06564	$C_6H_{11}O_6Na$	0.48	203.0521	232.4	337.8	264.7	439.4	228.5	623.9
7	L-Phenylalanine	HMDB00159	$C_9H_{11}NO_2$	0.86	166.0862	59.1	93.0	87.8	62.3	96.1	143.8
8	L-Leucine	HMDB00687	$C_6H_{13}NO_2$	0.82	132.1020	27.0	53.4	35.8	53.4	46.4	109.9
9	Choline	HMDB00097	$C_5H_{14}NO$	0.52	104.1067	18.5	36.5	32.5	38.0	21.0	87.5
10	Lyso-PC (C18:1)	HMDB02815	$C_{26}H_{52}NO_7P$	2.08	522.3589	24.3	0.9	0.3	8.4	14.9	42.2
11	Lyso-PC (C20:4)	HMDB10395	$C_{28}H_{50}NO_7P$	1.95	544.3401	33.4	0.2	0.2	9.6	14.9	9.3
12	Lyso-PC (C22:6)	HMDB10404	$C_{30}H_{50}NO_7P$	1.92	568.3400	7.9	0.0	0.4	1.3	2.6	1.4

Metabolites were validated by comparing the LC-MS spectrum of the candidate metabolite with the spectrum of the corresponding pure standard and website database. Alternatively, the metabolites were validated by LC-MS analysis. The compound numbers given in the left column correspond to the peaks numbered in Fig. 1. The numbers given within parentheses in the "Compound" column correspond respectively to the number of carbons and double bonds found in the fatty acid molecule. Ion intensity for each compound was normalized by multiplying the ion intensity of each entry by the average of total ion intensities for the six samples shown, and then dividing by the sum of ion intensities for the corresponding sample. The compounds were ranked based on the sum of ion intensity of each compound. ESI, electrospray ionization; Gr., granules; HMDB, Human Metabolome Database; ID, identification; MG, mono-acylglycerol; NPs, nanoparticles; PC, phosphatidylcholine; RT, retention time (min).

HS or FBS since these proteins may interfere with the metabolomics methodology used (ESI Table S1,† "Trypsin" columns). We observed that the ion intensity of most validated metabolites identified in trypsin-serum NPs was comparable to that obtained for NPs prepared in untreated serum.

Heat maps of the metabolites identified in mineralo-organic NPs were used to illustrate the differences in metabolite intensities between samples (Fig. 2). In ESI^+ mode, FBS-NPs and HS-NPs formed a group that shared a common embranchment with HS granules (Fig. 2A, see the grouping

Table 2 List of validated organic compounds identified in mineralo-organic NPs and serum granules in the ESI$^-$ mode

#	Compound	ID number	Formula	RT	*m/z*	HS-NPs	Saliva-NPs	Urine-NPs	FBS-NPs	HS-Gr.	FBS-Gr.
13	Stearic acid (C18:0)	HMDB00827	$C_{18}H_{36}O_2$	2.81	283.2624	13746.4	15853.4	16297.9	14789.5	14370.6	15433.7
14	Palmitic acid (C16:0)	HMDB00220	$C_{16}H_{32}O_2$	2.50	255.2313	14136.1	12526.1	11878.9	14216.3	13926.4	7928.0
15	Myristic acid (C14:0)	HMDB00806	$C_{14}H_{28}O_2$	2.28	227.2004	2213.9	1893.9	1971.8	1961.3	2120.9	2614.4
16	Margaric acid (C17:0)	HMDB02259	$C_{17}H_{34}O_2$	2.66	269.2473	1401.4	2085.1	2110.9	1278.2	1104.5	1162.6
17	Oleic acid (C18:1)	HMDB00207	$C_{18}H_{34}O_2$	2.52	281.2482	1232.9	1027.5	978.7	1018.7	1439.2	2584.7
18	Pentadecanoic acid (C15:0)	HMDB00826	$C_{15}H_{30}O_2$	2.39	241.2156	1187.7	824.7	989.3	878.6	906.9	1832.7
19	Palmitoleic acid (C16:1)	HMDB03229	$C_{16}H_{30}O_2$	2.31	253.2156	740.6	652.2	602.2	663.7	774.7	2338.9
20	Linolenic acid (C18:3)	HMDB00673	$C_{18}H_{32}O_2$	2.34	279.2319	298.8	166.3	164.3	217.3	363.0	427.2
21	Arachidic acid (C20:0)	HMDB02212	$C_{20}H_{40}O_2$	3.32	311.2951	146.2	216.4	180.9	150.8	117.7	643.4
22	9-Heptadecenoic acid (C17:0)	HMDB31046	$C_{17}H_{32}O_2$	2.40	267.2322	149.5	117.7	113.1	111.8	162.5	323.9
23	Lyso-PC (C18:2)	HMDB10386	$C_{27}H_{48}N_7O_4P$	2.18	564.3426	135.0	79.4	154.8	136.2	70.1	99.9
24	Arachidonic acid (C20:4)	HMDB01043	$C_{20}H_{32}O_2$	2.27	303.2306	52.2	4.9	5.0	22.8	77.6	53.6
25	DHA (C22:6)	HMDB02183	$C_{22}H_{32}O_2$	2.21	327.2319	7.6	0.9	0.6	3.4	14.6	5.4

Metabolites were validated by comparing the LC-MS spectrum of the candidate metabolite with the spectrum of the corresponding pure standard and website database. Alternatively, the metabolites were validated by LC-MS analysis. The compound numbers given in the left column correspond to the peaks numbered in Fig. 1. The numbers given within parentheses in the "Compound" column correspond respectively to the number of carbons and double bonds found in the fatty acid molecule. Ion intensity for each compound was normalized by multiplying the ion intensity of each entry by the average of total ion intensities for the six samples shown, and then dividing by the sum of ion intensities for the corresponding sample. The compounds were ranked based on the sum of ion intensity of each compound. DHA, docosahexaenoic acid; ESI, electrospray ionization; Gr., granules; HMDB, Human Metabolome Database; ID, identification; NPs, nanoparticles; PC, phosphatidylcholine; RT, retention time (min).

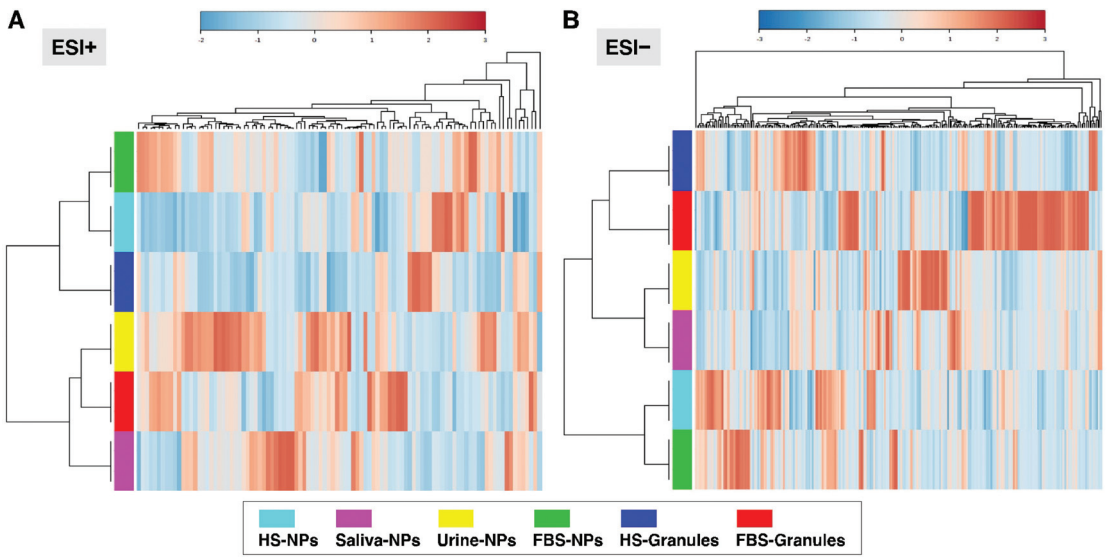

Fig. 2 Heat map diagrams of metabolites identified in the organic corona of mineralo-organic NPs and granules. Mineralo-organic NPs and serum granules were prepared and processed as described in Fig. 1 and Experimental procedure. Mineralo-organic NPs and granules were analyzed in (A) ESI$^+$ and (B) ESI$^-$ modes. Each heat map entry represents average values of six samples prepared in the same manner. The diagrams show the color-based intensity (legend on top) of metabolite candidates (dendrogram on top) and their grouping based on the similarity between specimens (dendrogram on the left).

shown on the left of heat maps). Another group was formed by urine NPs, FBS granules and saliva NPs, but the latter sample formed a sub-division separated from urine NPs and FBS granules. In heat maps of the ESI$^-$ analysis, HS and FBS granules formed a group showing the highest level of similarity with urine and saliva NPs (Fig. 2B). HS-NPs and FBS-NPs formed a separate group showing similar compound intensities.

We also performed a second, non-directed analysis of mineral NP samples using principal component analysis (PCA). As expected, sample replicates of both ESI$^+$ and ESI$^-$ modes formed clusters, confirming the reliability of the analysis performed (Fig. 3A and B). Notably, saliva and urine NPs analyzed in the ESI$^+$ mode clustered with FBS-NPs, while the other samples formed distinct groups that, in some cases,

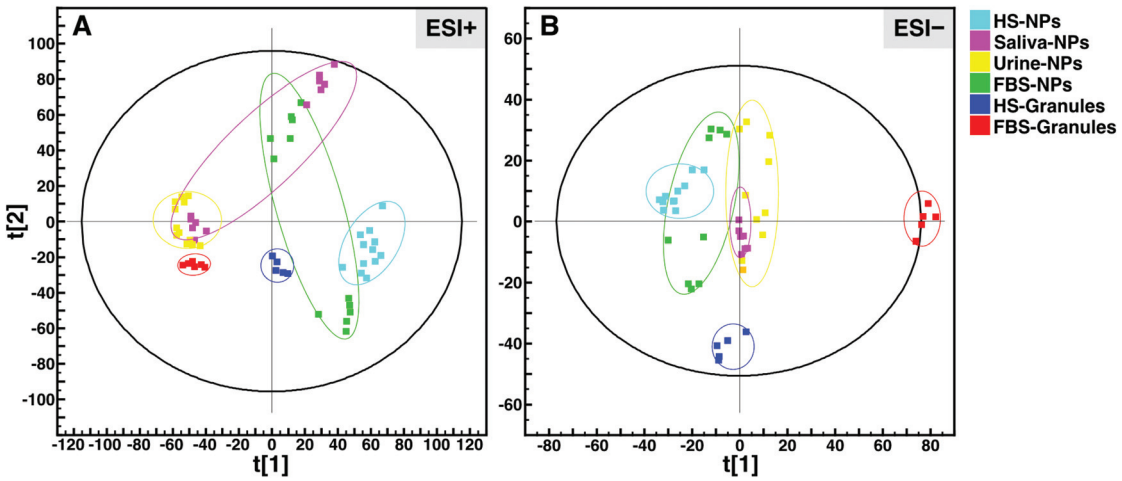

Fig. 3 PCA analysis of mineralo-organic NPs and serum granules derived from body fluids. Mineralo-organic NPs and granules were prepared and processed as described in Fig. 1 (see also Experimental procedure). The samples were analyzed in (A) ESI^+ and (B) ESI^- modes. The diagrams illustrate the similarities in the metabolite candidates identified in the various specimens represented by squares.

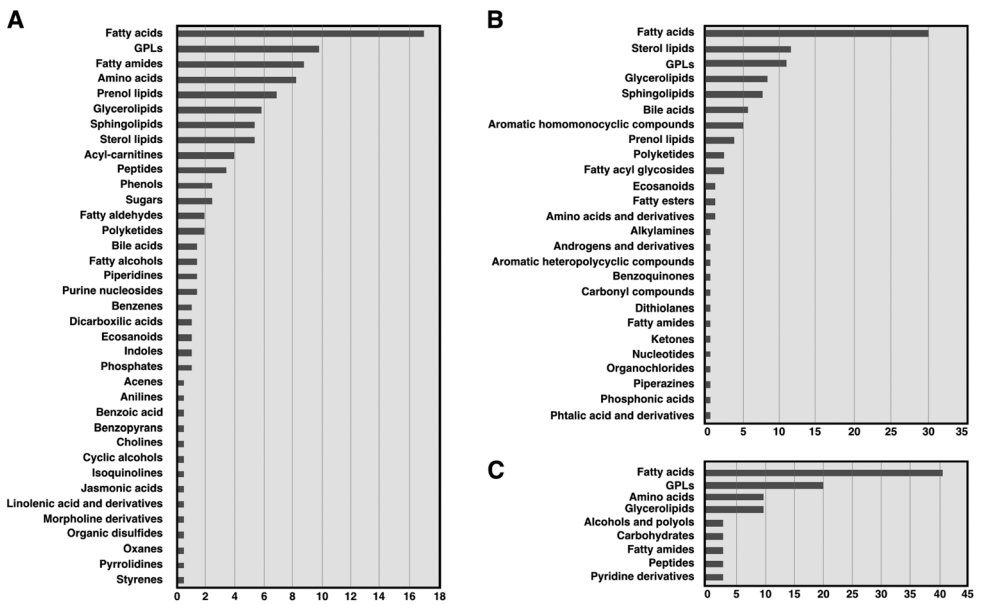

Fig. 4 Chemical classification of metabolites bound to mineralo-organic NPs and serum granules. (A) Non-validated metabolites identified in ESI^+ mode. (B) Non-validated metabolites identified in ESI^- mode. (C) Validated metabolites identified in ESI^+ and ESI^- modes. The *X* axis of each graph represents percentages. The metabolites shown in (A and B) correspond to the ones listed in ESI Table S1,† while the compounds shown in (C) are listed in Tables 1 and 2. Metabolites were classified based on chemical classes provided in the Human Metabolome Database (HMDB).

overlapped with FBS-NPs (Fig. 3A). In the ESI^- mode, FBS-NPs, urine NPs and saliva NPs partially overlapped (Fig. 3B). In addition, HS-NPs partially overlapped with FBS-NPs while FBS granules and HS granules formed two distinct clusters (Fig. 3B).

The organic compounds identified in mineralo-organic NPs and granules belonged to a wide range of chemical classes (Fig. 4). For the metabolite candidates, the major chemical classes consisted of fatty acids, GPLs, sterol lipids, fatty amides, amino acids, prenol lipids and glycerolipids (Fig. 4A and B). For the validated compounds, fatty acids, GPLs, amino acids, and glycerolipids represented the most abundant metabolites identified (Fig. 4C).

We also analyzed the organic corona of calcium phosphate NPs prepared in human plasma (Fig. S3†). The organic compounds identified, which included lyso-PCs and fatty acids, were highly similar to the compounds identified in HS-NPs (ESI Tables S2 and S3†). Accordingly, heat maps showed that

plasma-NPs clustered with HS-NPs (Fig. S4†). PCA analysis indicated that the metabolites from plasma-NPs and HS-NPs overlapped in the ESI^- mode, while two distinct groups were formed in the ESI^+ mode (Fig. S5†).

To study the organic corona of synthetic NPs (SNPs), we analyzed the metabolites bound to polystyrene NPs incubated into HS (Fig. S3†). The metabolite profiles of polystyrene particles of 50 nm and 100 nm were highly comparable, both in terms of the identity and intensity of the metabolites found (ESI Tables S2 and S3†). Heat maps and PCA graphs also confirmed the high level of homology between the organic compounds bound to the particles of 50 and 100 nm (Fig. S4 and S5†). Notably, similar organic compounds were identified for the mineralo-organic HS-NPs and SNPs studied here (ESI Tables S2 and S3†).

Discussion

While advances have been made recently concerning the analysis of the protein corona of NPs and nanomaterials, the possibility that NPs may also harbor an organic corona had not been examined. Using a comprehensive metabolomics methodology, we identify here a wide range of metabolites that bind to mineralo-organic NPs derived from human body fluids and to synthetic NPs incubated in serum. The main compounds that bind to the mineral and synthetic NPs represent saturated free fatty acids such as stearic acid, palmitic acid, and myristic acid. In the blood, fatty acids of short and medium length may be transported by serum albumin, a protein which has been repeatedly found in association with the mineralo-organic NPs studied here.[2,4] These observations suggest that mineralo-organic NPs that form spontaneously in body fluids may act as carrier of organic molecules in body fluids. The formation of mineralo-organic NPs in human body fluids may therefore influence the concentrations of bound metabolites. The present study provides a platform to examine this possibility and to characterize the effect of the organic corona of NPs and nanomaterials.

The similarities between the organic composition of the mineralo-organic NPs prepared by addition of precipitating ions and the mineral granules isolated directly from serum support the physiological relevance of the approach used in the present study. In addition, the metabolomics analysis performed here may be used to analyze the metabolite composition of both synthetic and natural nanoparticles, including those destined to be injected in the human body for medical applications. We propose that the major organic compounds identified might serve as markers to follow the formation of mineralo-organic NPs formed in the human body.

A recent landmark study by Psychogios *et al.* reported a comprehensive analysis of the human serum metabolome using a variety of analytical chemistry techniques, including nuclear magnetic resonance (NMR) spectroscopy and LC-MS/MS.[33] The serum metabolome was found to contain 4429 metabolites, with the most abundant compounds being di- and triglycerides, phospholipids, fatty acids, steroids and their derivatives, amino acids, D-glucose, glycerol, lactate, urea, and creatinine. Our analysis of the organic corona of mineralo-organic NPs is consistent with this serum metabolome study as the corona compounds consisted of similar molecules, including fatty acids, lipids, sugars, and amino acids (Tables 1 and 2 and ESI Table S1†). On the other hand, di- and triglycerides may not bind effectively to mineralo-organic NPs in view of the bulky structure of these compounds. In comparison to whole serum, some compounds such as fatty acids may be enriched on the surface of the particles, possibly affecting the biodistribution and function of the compounds *in vivo*.

The observation that several lipids (see Tables 1 and 2) and apolipoproteins (see previous studies[2,3]) bind to mineralo-organic NPs suggest that mineral particles may be analogous to the lipoproteins that transport lipids in body fluids, a possibility noted previously by other authors.[31,34,35] For instance, the observation that mineralo-organic NPs bind to apo-A1,[2] which is usually found in association with high-density lipoproteins (HDL) suggests that the mineral particles may have a biodistribution similar to that of HDL *in vivo*. Given that mineralo-organic NPs may also bind to other apolipoproteins such as apo-B100,[2] which is associated with low density lipoproteins (LDL), it is also possible that the biodistribution of these mineral particles may depend on the nature of the various bound lipoproteins *in vivo*.

We also observed the potential presence of nucleosides and nucleotide derivatives within the mineralo-organic NPs (ESI Table S1,† compounds 162, 217, and 343 in ESI^+ mode and 236 in ESI^-). This observation suggests that DNA may bind to the particles described here. Accordingly, DNA molecules present in body fluids (possibly originating from dead cells or microbes) may be loaded onto mineralo-organic NPs, a possibility which remains to be examined in more detail.

The observation that several organic metabolites bind to mineralo-organic NPs suggests that these compounds may inhibit particle formation and growth, as seen for proteins.[2] Jahnen-Dechent *et al.* proposed that serum proteins like fetuin-A may act as chaperones that bind excess mineral in body fluids, and might give the particles a soluble form, prevent their growth, and allow excretion *via* urine or phagocytosis by macrophages.[36] These researchers showed that mineral NPs injected intravenously into mice are rapidly removed from the circulation by macrophages of the liver and spleen *via* the scavenger receptor.[37] The possibility that binding of the organic molecules identified here may prevent further ion deposition and particle aggregation remains to be examined.

A recent study showed that gold NPs coated with polymers partially lose their polymer shell when the particles are injected intravenously into rats.[38] Degradation of the polymer shell was attributed to proteolytic enzymes found in the liver. This study suggests that the organic corona of biological and synthetic NPs may be a dynamic entity whose composition is modulated by various factors *in vivo*. Time-dependent monitoring of the organic corona of particles found in the body may

therefore be necessary to address the dynamic nature of this process.

Conclusion

Our results suggest that the concept of the protein corona, which has been shown to determine the effects and distribution of NPs in the human body, should now be extended to organic molecules, including metabolites. The metabolomics methodology described here should prove useful for the analysis of synthetic and natural NPs that interact with the human body.

Acknowledgements

This study was supported by Primordia Institute of New Sciences and Medicine and by grants from Chang Gung University (FMRPD2T02), Ming Chi University of Technology (0XB0), and the Ministry of Education of Taiwan, ROC (EMRPD190041).

References

1 J. Martel and J. D. Young, *Proc. Natl. Acad. Sci. U. S. A.*, 2008, **105**, 5549–5554.
2 J. D. Young, J. Martel, L. Young, C. Y. Wu, A. Young and D. Young, *PLoS One*, 2009, **4**, e4417.
3 J. D. Young, J. Martel, D. Young, A. Young, C. M. Hung, L. Young, Y. J. Chao, J. Young and C. Y. Wu, *PLoS One*, 2009, **4**, e5421.
4 C. Y. Wu, J. Martel, D. Young and J. D. Young, *PLoS One*, 2009, **4**, e8058.
5 J. D. Young and J. Martel, *Sci. Am.*, 2010, **302**, 52–59.
6 J. Martel, C. Y. Wu and J. D. Young, *PLoS One*, 2010, **5**, e10343.
7 J. Martel, D. Young, A. Young, C. Y. Wu, C. D. Chen, J. S. Yu and J. D. Young, *Anal. Biochem.*, 2011, **418**, 111–125.
8 H. H. Peng, J. Martel, Y. H. Lee, D. M. Ojcius and J. D. Young, *Nanomedicine*, 2011, **6**, 643–658.
9 J. Martel, D. Young, H. H. Peng, C. Y. Wu and J. D. Young, *Ann. Rev. Earth Planet. Sci.*, 2012, **40**, 167–193.
10 H. H. Peng, C. Y. Wu, D. Young, J. Martel, A. Young, D. M. Ojcius, Y. H. Lee and J. D. Young, *Small*, 2013, **9**, 2297–2307.
11 C. Y. Wu, J. Martel, W. C. Cheng, C. C. He, D. M. Ojcius and J. D. Young, *J. Biol. Chem.*, 2013, **288**, 30571–30584.
12 C. Y. Wu, L. Young, D. Young, J. Martel and J. D. Young, *PLoS One*, 2013, **8**, e75501.
13 J. Martel, H. H. Peng, D. Young, C. Y. Wu and J. D. Young, *Nanomedicine*, 2014, **9**, 483–499.
14 C. Y. Wu, D. Young, J. Martel and J. D. Young, *Nanomedicine*, 2015, **10**, 2659–2676.
15 T. Y. Wong, C. Y. Wu, J. Martel, C. W. Lin, F. Y. Hsu, P. Y. Lin and J. D. Young, *Sci. Rep.*, 2015, **5**, 15272.
16 T. Y. Wong, H. H. Peng, C. Y. Wu, J. Martel, D. M. Ojcius, F. Y. Hsu and J. D. Young, *Nanomedicine*, 2015, **10**, 3519–3535.
17 E. O. Kajander, I. Kuronen, K. Akerman, A. Pelttari and N. Ciftcioglu, *Proc. Soc. Photo-Opt. Instrum. Eng.*, 1997, **3111**, 420–428.
18 E. O. Kajander and N. Ciftcioglu, *Proc. Natl. Acad. Sci. U. S. A.*, 1998, **95**, 8274–8279.
19 N. Ciftcioglu, D. S. McKay, G. Mathew and E. O. Kajander, *J. Invest. Med.*, 2006, **54**, 385–394.
20 I. Lynch and K. A. Dawson, *Nano Today*, 2008, **3**, 40–47.
21 A. E. Nel, L. Madler, D. Velegol, T. Xia, E. M. Hoek, P. Somasundaran, F. Klaessig, V. Castranova and M. Thompson, *Nat. Mater.*, 2009, **8**, 543–557.
22 M. P. Monopoli, C. Aberg, A. Salvati and K. A. Dawson, *Nat. Nanotechnol.*, 2012, **7**, 779–786.
23 D. Docter, D. Westmeier, M. Markiewicz, S. Stolte, S. K. Knauer and R. H. Stauber, *Chem. Soc. Rev.*, 2015, **44**, 6094–6121.
24 M. I. Setyawati, C. Y. Tay, D. Docter, R. H. Stauberb and D. T. Leong, *Chem. Soc. Rev.*, 2015, **44**, 8174–8199.
25 C. D. Walkey, J. B. Olsen, F. Song, R. Liu, H. Guo, D. W. Olsen, Y. Cohen, A. Emili and W. C. Chan, *ACS Nano*, 2014, **8**, 2439–2455.
26 T. Cedervall, I. Lynch, S. Lindman, T. Berggard, E. Thulin, H. Nilsson, K. A. Dawson and S. Linse, *Proc. Natl. Acad. Sci. U. S. A.*, 2007, **104**, 2050–2055.
27 S. Tenzer, D. Docter, J. Kuharev, A. Musyanovych, V. Fetz, R. Hecht, F. Schlenk, D. Fischer, K. Kiouptsi, C. Reinhardt, K. Landfester, H. Schild, M. Maskos, S. K. Knauer and R. H. Stauber, *Nat. Nanotechnol.*, 2013, **8**, 772–781.
28 Y. Yan, K. T. Gause, M. M. Kamphuis, C. S. Ang, N. M. O'Brien-Simpson, J. C. Lenzo, E. C. Reynolds, E. C. Nice and F. Caruso, *ACS Nano*, 2013, **7**, 10960–10970.
29 W. Jiang, K. Lai, Y. Wu and Z. Gu, *Arch. Pharmacal Res.*, 2014, **7**, 129–141.
30 S. Wan, P. M. Kelly, E. Mahon, H. Stockmann, P. M. Rudd, F. Caruso, K. A. Dawson, Y. Yan and M. P. Monopoli, *ACS Nano*, 2015, **9**, 2157–2166.
31 E. Hellstrand, I. Lynch, A. Andersson, T. Drakenberg, B. Dahlbäck, K. A. Dawson, S. Linse and T. Cedervall, *FEBS J.*, 2009, **276**, 3372–3381.
32 J. Xia, R. Mandal, I. V. Sinelnikov, D. Broadhurst and D. S. Wishart, *Nucleic Acids Res.*, 2012, **40**, W127–W133.
33 N. Psychogios, D. D. Hau, J. Peng, A. C. Guo, R. Mandal, S. Bouatra, I. Sinelnikov, R. Krishnamurthy, R. Eisner, B. Gautam, N. Young, J. Xia, C. Knox, E. Dong, P. Huang, Z. Hollander, T. L. Pedersen, S. R. Smith, F. Bamforth, R. Greiner, B. McManus, J. W. Newman, T. Goodfriend and D. S. Wishart, *PLoS One*, 2011, **6**, e16957.
34 P. C. Rensen, R. L. de Vrueh, J. Kuiper, M. K. Bijsterbosch, E. A. Biessen and T. J. van Berkel, *Adv. Drug Delivery Rev.*, 2001, **47**, 251–276.
35 N. S. Chung and K. M. Wasan, *Adv. Drug Delivery Rev.*, 2004, **56**, 1315–1334.

36 W. Jahnen-Dechent, C. Schäfer, M. Ketteler and M. D. McKee, *J. Mol. Med.*, 2008, **86**, 379–389.
37 M. Herrmann, C. Schäfer, A. Heiss, S. Gräber, A. Kinkeldey, A. Büscher, M. M. Schmitt, J. Bornemann, F. Nimmerjahn, M. Herrmann, L. Helming, S. Gordon and W. Jahnen-Dechent, *Circ. Res.*, 2012, **111**, 575–584.
38 W. G. Kreyling, A. M. Abdelmonem, Z. Ali, F. Alves, M. Geiser, N. Haberl, R. Hartmann, S. Hirn, D. J. de Aberasturi, K. Kantner, G. Khadem-Saba, J. M. Montenegro, J. Rejman, T. Rojo, I. R. de Larramendi, R. Ufartes, A. Wenk and W. J. Parak, *Nat. Nanotechnol.*, 2015, **10**, 619–623.

Electronic Supplementary Material (ESI) for Nanoscale.

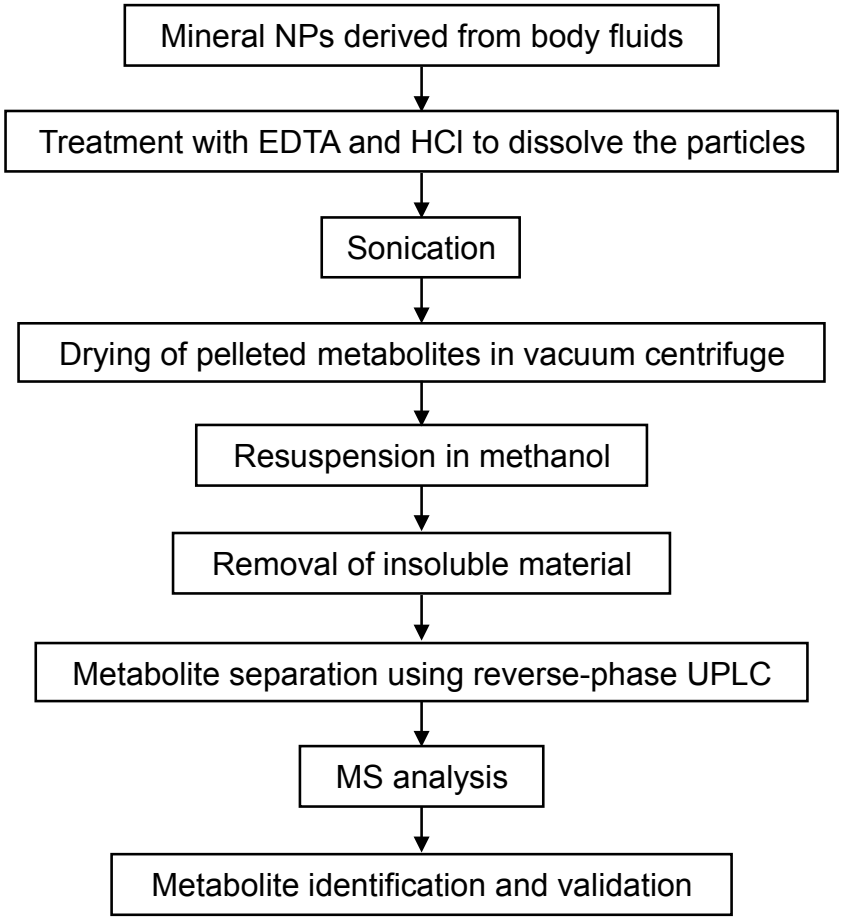

Fig. S1 Strategy used to determine the metabolite composition of mineral-organic NPs and granules. Washed mineralo-organic NPs were treated with 50 mM EDTA and 0.1 M HCl to dissolve the particles and release metabolites. The metabolites were separated on a reverse-phase LC column and submitted to LC-MS analysis as described in Experimental procedure.

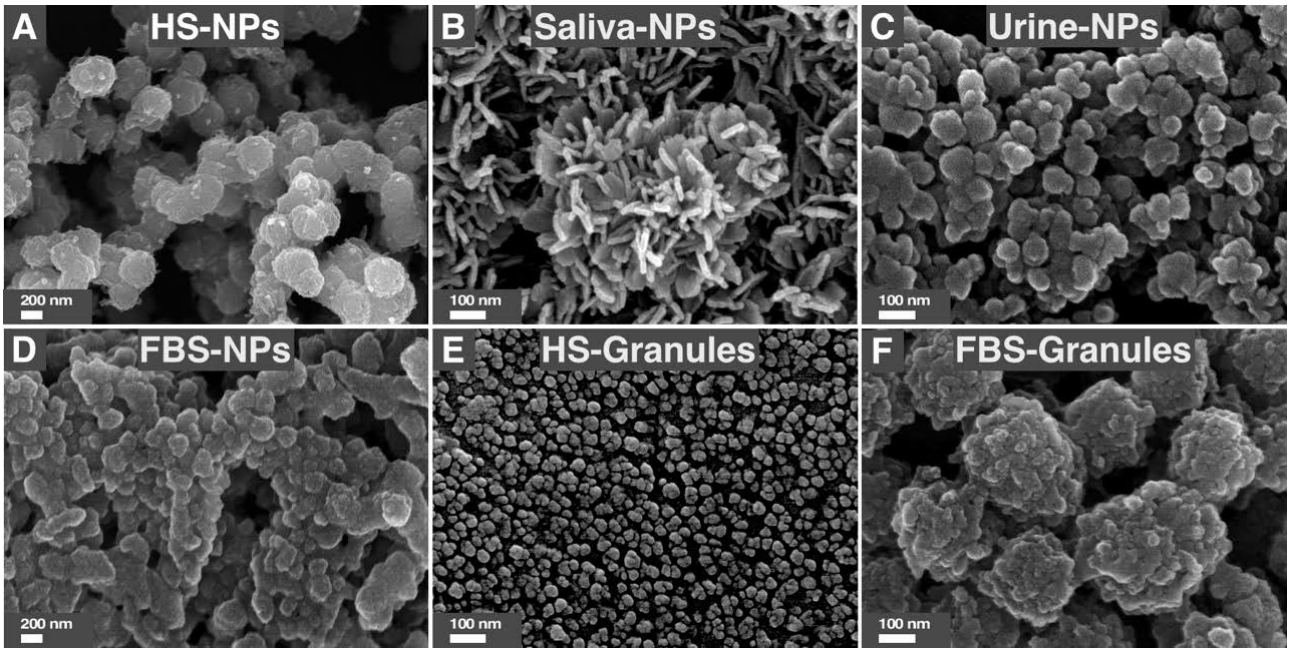

Fig. S2 Scanning electron microscopy (SEM) images of particles used in the present study. Samples were prepared for SEM observation as described in Experimental procedure. All particles show a round morphology, except for saliva-NPs which have a bacillus-like shape (B). Particle sizes are as follows: (A) 100±300 nm; (C) 50±200 nm; (D) 100±200 nm; (E) 20±50 nm; (F) 20±300 nm. Bacillus-like particles in (B) were 100±50 nm long and 20±20 nm large.

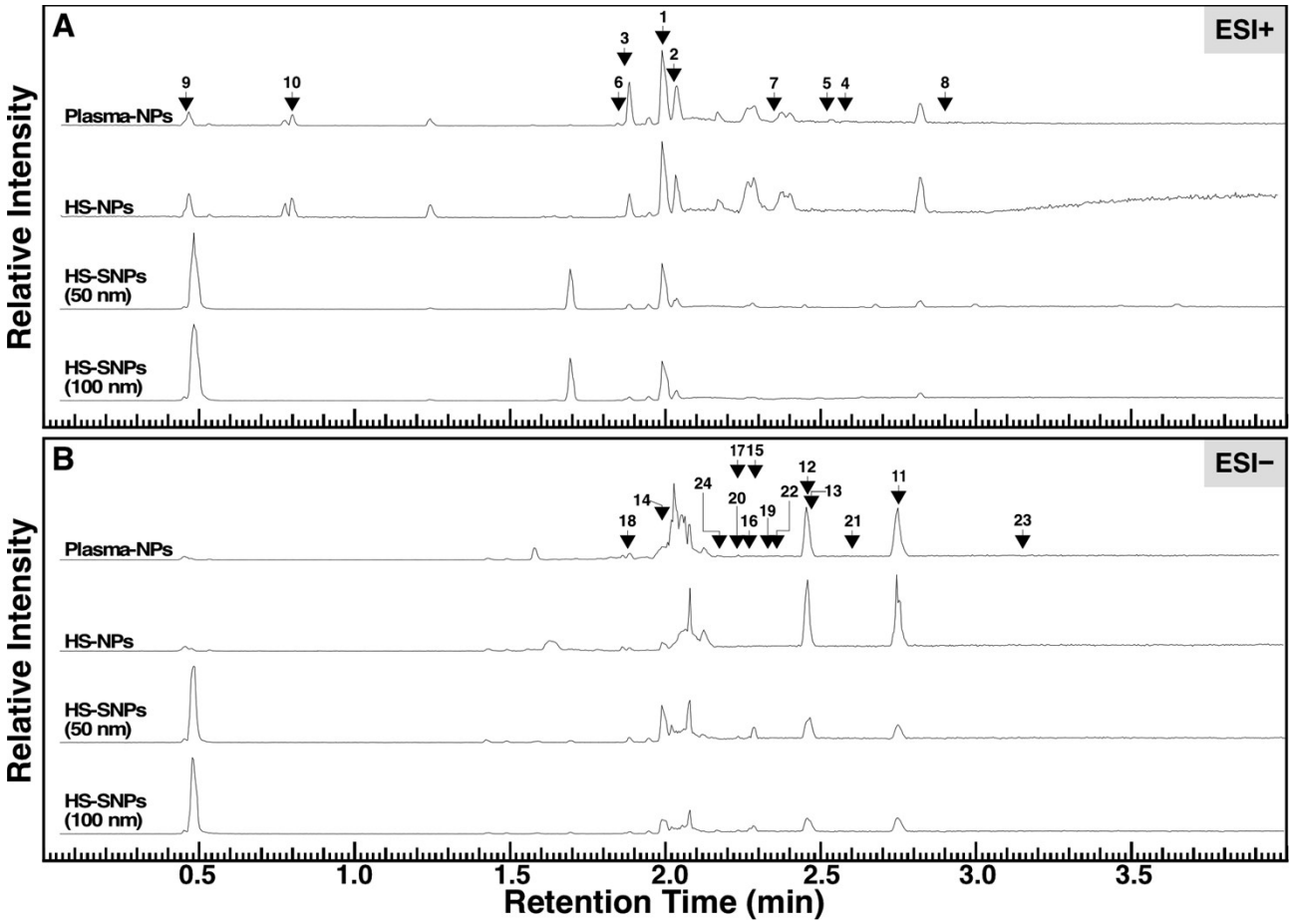

Fig. S3 LC/MS chromatograms of biological and synthetic NPs prepared in human body fluids. Calcium phosphate NPs ("Plasma-NPs" and "HS-NPs") were prepared by adding $CaCl_2$ and NaH_2PO_4 at 3 mM each in DMEM containing human plasma or human serum (HS), prior to incubation overnight and preparation for LC/MS analysis. Commercial synthetic NPs (SNPs) with a diameter of 50 or 100 nm were incubated into HS and prepared for LC/MS analysis as described in Experimental procedure. Samples were analyzed in (A) ESI^+ and (B) ESI^- modes. Peak numbers correspond to the compounds listed in Supplementary Tables S1 and S2.

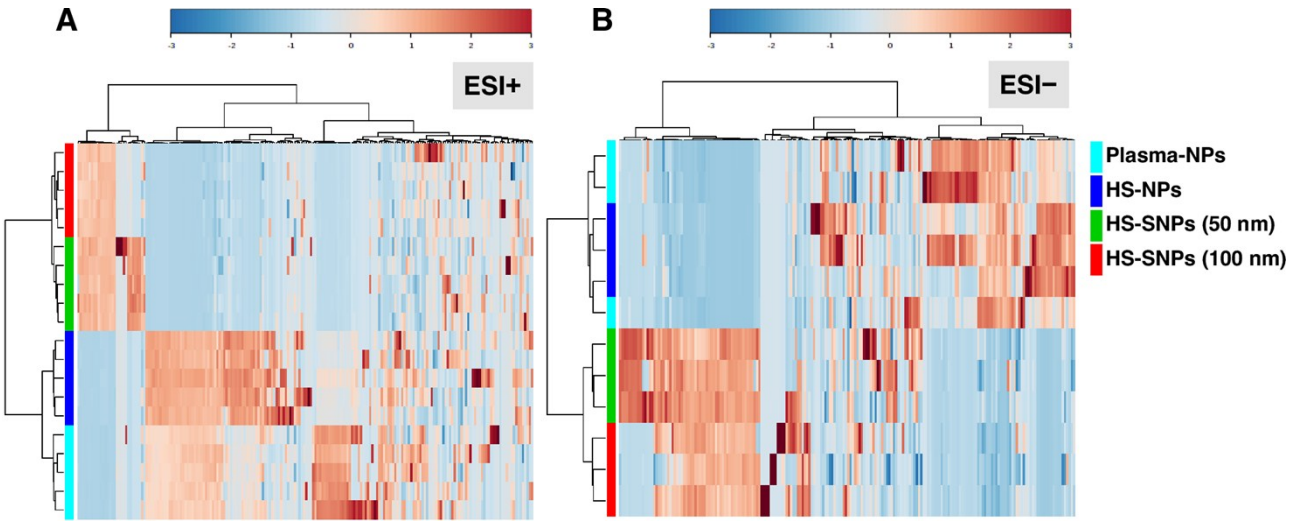

Fig. S4 Heat map diagrams of metabolites identified in the organic corona of biological and synthetic NPs. Calcium phosphate NPs ("Plasma-NPs" and "HS-NPs") were prepared and processed as described in Supplementary Fig. S3 and Experimental procedure. Synthetic NPs (SNPs) of 50 or 100 nm were incubated into HS and prepared for LC/MS analysis as described in Experimental procedure. Particle specimens were analyzed in (A) ESI^+ and (B) ESI^- modes. For each sample, 3–5 specimens were prepared and analyzed in the same manner. The diagrams illustrate the color-based intensity (legend on top) for the various metabolite candidates (dendrogram on top) and their grouping based on the specimens analyzed (dendrogram on the left).

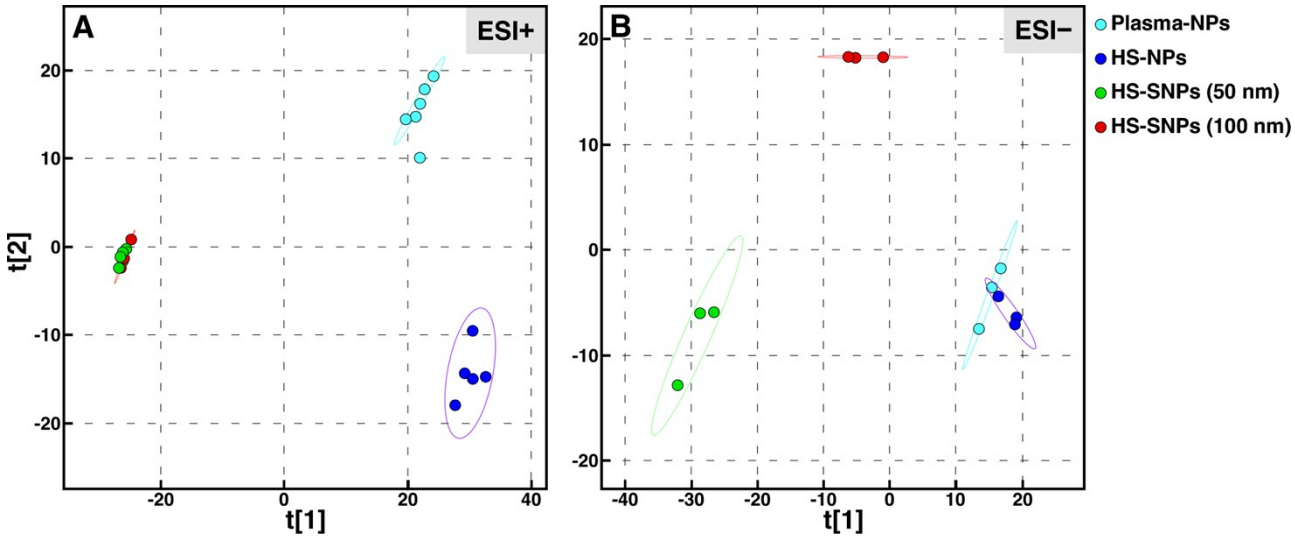

Fig. S5 PCA analysis of biological and synthetic NPs prepared in human body fluids. Calcium phosphate NPs ("Plasma-NPs" and "HS-NPs") were prepared and processed as described in Supplementary Fig. S3 (see also Experimental procedure). Synthetic NPs (SNPs) of 50 or 100 nm were incubated into HS and prepared for LC/MS analysis as described in Experimental procedure. Samples were analyzed in (A) ESI^+ and (B) ESI^- modes. The diagrams illustrate the level of similarity between the metabolite candidates identified in the samples (represented by circles).

Table S2 List of validated organic compounds identified in mineralo-organic particles and synthetic nanoparticles in the ESI^+ mode

#	Compound	ID Number	Formula	RT	*m/z*	Plasma-NPs	HS-NPs	50-nm SNPs	100-nm SNPs
1	Lyso-PC (16:0)	HMDB10382	$C_{24}H_{50}NO_7P$	1.99	496.3409	94.3	91.2	75.4	75.3
2	Lyso-PC (18:1)	HMDB02815	$C_{26}H_{52}NO_7P$	2.03	522.3556	25.2	31.0	46.7	45.8
3	Lyso-PC (20:4)	HMDB10395	$C_{28}H_{50}NO_7P$	1.87	544.3392	3.2	1.6	2.4	1.5
4	MG (18:0)	HMDB11535	$C_{21}H_{42}O_4$	2.58	359.3133	0.2	0.3	0.6	1.9
5	Stearamide	HMDB34146	$C_{18}H_{37}NO$	2.52	284.2955	2.0	0.7	–	–
6	Lyso-PC (22:6)	HMDB10404	$C_{30}H_{50}NO_7P$	1.85	568.3407	0.7	0.4	0.8	0.3
7	MG (16:0)	HMDB11564	$C_{19}H_{38}O_4$	2.35	331.2856	0.2	0.3	0.1	1.1
8	MG (18:2)	HMDB11538	$C_{21}H_{38}O_4$	2.58	355.0718	–	0.5	–	–
9	Glucose	HMDB06564	$C_6H_{11}O_6Na$	0.46	203.0525	0.3	0.1	–	–
10	Niacinamide	HMDB01406	$C_6H_6N_2O$	0.80	123.0550	–	–	–	–

Metabolites were validated by comparing the LC-MS spectrum of the candidate metabolite with the spectrum of the corresponding pure standard and website database. Alternatively, the metabolites were validated by LC-MS analysis. The compound numbers given in the left column correspond to the peaks numbered in Fig. S3. The numbers given within parentheses in the "Compound" column correspond respectively to the number of carbons and double bonds found in the fatty acid molecule. Ion intensity for each compound was normalized by multiplying the ion intensity of each entry by the average of total ion intensities for the six samples shown, and then dividing by the sum of ion intensities for the corresponding sample. The compounds were ranked based on the sum of ion intensity of each compound. ESI, electrospray ionization; HMDB, Human Metabolome Database; ID, identification; MG, monoacylglycerol; NPs, nanoparticles; PC, phosphatidylcholine; RT, retention time (min), SNPs, synthetic nanoparticles.

Table S3 List of validated organic compounds identified in mineralo-organic particles and synthetic nanoparticles in the ESI^- mode

#	Compound	ID Number	Formula	RT	*m/z*	Plasma-NPs	HS-NPs	50-nm SNPs	100-nm SNPs
11	Stearic acid (C18:0)	HMDB00827	$C_{18}H_{36}O_2$	2.75	283.2629	46.4	35.5	74.4	56.2
12	Palmitic acid (C16:0)	HMDB00220	$C_{16}H_{32}O_2$	2.46	255.2310	34.0	33.9	61.2	78.3
13	Oleic acid (C18:1)	HMDB00207	$C_{18}H_{34}O_2$	2.47	281.2459	34.0	41.5	23.0	27.4
14	Lyso-PC (16:0)	HMDB10382	$C_{24}H_{50}NO_7P$	1.99	480.3090	21.1	23.1	7.2	5.7
15	Linolenic acid (C18:3)	HMDB00673	$C_{18}H_{32}O_2$	2.29	279.2304	15.8	20.7	5.4	5.6
16	Palmitoleic acid (C16:1)	HMDB03229	$C_{16}H_{30}O_2$	2.27	253.2148	12.3	10.4	4.5	4.6
17	Myristic acid (C14:0)	HMDB00806	$C_{14}H_{28}O_2$	2.23	227.2000	7.7	7.7	5.4	6.0
18	Lyso-PC (18:2)	HMDB10386	$C_{27}H_{48}N_7O_4P$	1.88	564.3318	4.9	5.6	7.1	3.6
19	Pentadecanoic acid (C15:0)	HMDB00826	$C_{15}H_{30}O_2$	2.33	241.2153	6.3	5.7	3.2	3.6
20	Arachidonic acid (C20:4)	HMDB01043	$C_{20}H_{32}O_2$	2.23	303.2317	4.6	5.8	0.8	0.9
21	Margaric acid (C17:0)	HMDB02259	$C_{17}H_{34}O_2$	2.60	269.2478	3.8	3.3	2.3	2.2
22	9-Heptadecenoic acid (C17:0)	HMDB31046	$C_{17}H_{32}O_2$	2.36	267.2328	3.7	1.7	0.4	1.0
23	Arachidic acid (C20:0)	HMDB02212	$C_{20}H_{40}O_2$	3.15	311.2960	1.2	0.5	1.7	1.5
24	DHA (C22:6)	HMDB02183	$C_{22}H_{32}O_2$	2.18	327.2342	1.3	1.7	0.5	0.6

Metabolites were validated by comparing the LC-MS spectrum of the candidate metabolite with the spectrum of the corresponding pure standard and website database. Alternatively, the metabolites were validated by LC-MS analysis. The compound numbers given in the left column correspond to the peaks numbered in Fig. S3. The numbers given within parentheses in the "Compound" column correspond respectively to the number of carbons and double bonds found in the fatty acid molecule. Ion intensity for each compound was normalized by multiplying the ion intensity of each entry by the average of total ion intensities for the six samples shown, and then dividing by the sum of ion intensities for the corresponding sample. The compounds were ranked based on the sum of ion intensity of each compound. DHA, docosahexaenoic acid; ESI, electrospray ionization; HMDB, Human Metabolome Database; ID, identification; NPs, nanoparticles; PC, phosphatidylcholine; RT, retention time (min), SNPs, synthetic nanoparticles.